Electronic Supplementary Material (ESI) for RSC Advances.

Zero-field Slow Relaxation of Magnetization in Cobalt(II) Single-ion Magnets: Suppression of Quantum Tunneling of Magnetization by Tailoring the Intermolecular Magnetic Coupling

Ryoji Mitsuhashi,[a]* Satoshi Hosoya,[b] Takayoshi Suzuki[c,d], Yukinari Sunatsuki,[c] Hiroshi Sakiyama,[e] and Masahiro Mikuriya[b]

[a] *Institute of Liberal Arts and Science, Kanazawa University, Kakuma, Kanazawa, Ishikawa 920-1192, Japan*

[b] *School of Science and Technology, Kwansei Gakuin University, 2-1 Gakuen, Sanda, Hyogo 669-1337, Japan*

[c] *Department of Chemistry, Faculty of Science, Okayama University, 3-1-1 Tsushima-naka, Kita-ku, Okayama 700-8530, Japan*

[d] *Research Institute for Interdisciplinary Science, Okayama University, 3-1-1 Tsushima-naka, Kita-ku, Okayama 700-8530, Japan*

[e] *Department of Science, Faculty of Science, Yamagata University, 1-4-12 Kojirakawa, Yamagata 990-8560, Japan*

Contents:

Fig. S3 Temperature dependence of (a) the in-phase χ'_M vs. frequency plots and (b) out-of-phase χ''_M vs. frequency plots for **1**·CH_3OH in 1.4 kOe dc field with ac frequency of 0.1–1488 Hz. The lines are a guide for the eye.
Fig. S4 Cole-Cole plot for **1**·CH_3OH in 1.4 kOe dc field from 1.9 to 6.5 K. The solid lines represent the fit to a generalized Debye model.
Table S7 Cole-Cole fit values for **1**·CH_3OH in 1.4 kOe dc field from 1.9 to 6.5 K.
Fig. S5 Temperature dependence of (a) the in-phase χ'_M vs. frequency plots and (b) out-of-phase χ''_M vs. frequency plots for **2** in 0 Oe dc field with ac frequency of 0.1–1488 Hz (1.9 K–8.0 K). The lines are a guide for the eye.
Fig. S6 Dc field dependence of (a) the in-phase χ'_M vs. frequency plots and (b) out-of-phase χ''_M vs. frequency plots for **2** with ac frequency of 0.1–148.8 Hz at 1.9 K. The lines are a guide for the eye.
Fig. S7 Temperature dependence of (a) the in-phase χ'_M vs. frequency plots and (b) out-of-phase χ''_M vs. frequency plots for **2** in 0.4 kOe dc field with ac frequency of 0.1–1488 Hz (1.9 K–8.0 K). The lines are a guide for the eye. The lines are a guide for the eye.
Fig. S8 Cole-Cole plot for **2** (a) in zero field and (b) in 0.4 kOe dc field from 1.9 to 8 K. The solid lines represent the fit to a generalized Debye model.
Table S8 Cole-Cole fit values for **2** in zero dc field from 1.9 to 8.0 K.
Table S9 Cole-Cole fit values for **2** in 0.4 kOe dc field from 1.9 to 8.0 K.
Fig. S9 Temperature dependence of (a) the in-phase χ'_M vs. frequency plots and (b) out-of-phase χ''_M vs. frequency plots for **3** in 0 Oe dc field with ac frequency of 1–1488 Hz (1.9 K–8.0 K). The lines are a guide for the eye.
Fig. S10 Dc field dependence of (a) the in-phase χ'_M vs. frequency plots and (b) out-of-phase χ''_M vs. frequency plots for **3** with ac frequency of 0.1–1488 Hz at 4 K. The lines are a guide for the eye.
Fig. S11 Temperature dependence of (a) the in-phase χ'_M vs. frequency plots and (b) out-of-phase χ''_M vs. frequency plots for **3** in 0.8 kOe dc field with ac frequency of 0.03–1488 Hz (2.8 K–8.0 K). The lines are a guide for the eye.
Fig. S12 Cole-Cole plot for **3** (a) in zero field and (b) in 0.8 kOe dc field from 1.9 to 8 K. The solid lines represent the fit to a generalized Debye model.
Table S10 Cole-Cole fit values for **3** in zero dc field from 1.9 to 8.0 K.
Table S11 Cole-Cole fit values for **3** in 0.8 kOe dc field from 2.8 to 8.0 K.
Fig. S13 Cole-Cole plot for **3** under 0.2–5.0 kOe. The solid lines represent the fit to a generalized Debye model.
Table S12 Cole-Cole fit values for **3** at 4 K with an applied dc field of 0.2 to 5.0 kOe.
Fig. S14 Temperature dependence of (a) the in-phase χ'_M vs. frequency plots and (b) out-of-phase χ''_M vs. frequency plots for **4**·CH_3OH in 0 Oe dc field with ac frequency of 1–1488 Hz (1.9 K–6.0 K). The lines are a guide for the eye.
Fig. S15 Dc field dependence of (a) the in-phase χ'_M vs. frequency plots and (b) out-of-phase χ''_M vs. frequency plots for **4**·CH_3OH with ac frequency of 1–1488 Hz at 3.4 K. The lines are a guide for the eye.

Fig. S16 Temperature dependence of (a) the in-phase χ'_M vs. frequency plots and (b) out-of-phase χ''_M vs. frequency plots for **4**·CH_3OH in 0.4 kOe dc field with ac frequency of 1–1488 Hz (1.9 K–6.0 K). The lines are a guide for the eye.

Fig. S17 Temperature dependence of (a) the in-phase χ'_M vs. frequency plots and (b) out-of-phase χ''_M vs. frequency plots for **4**·CH_3OH in 1.8 kOe dc field with ac frequency of 0.1–1488 Hz (1.9 K–7.0 K). The lines are a guide for the eye.

Fig. S18 Cole-Cole plot for **4**·CH_3OH (a) in zero field from 1.9 to 6 K, (b) in 0.4 kOe dc field from 1.9 to 6 K and (c) in 1.8 Oe dc field from 1.9 to 7 K. The solid lines represent the fit to a generalized Debye model.

Table S13 Cole-Cole fit values for **4**·CH_3OH in zero dc field from 1.9 to 6.0 K.

Table S14 Cole-Cole fit values for **4**·CH_3OH in 0.4 kOe dc field from 1.9 to 6.0 K.

Table S15 Cole-Cole fit values for **4**·CH_3OH in 1.8 kOe dc field from 1.9 to 7.0 K.

Fig. S19 Temperature dependence of (a) the in-phase χ'_M vs. frequency plots and (b) out-of-phase χ''_M vs. frequency plots for **1'$_{0.33}$**·CH_3OH in 0 kOe dc field with ac frequency of 1–1488 Hz (1.9 K–2.6 K). The lines are a guide for the eye.

Fig. S20 Temperature dependence of (a) the in-phase χ'_M vs. frequency plots and (b) out-of-phase χ''_M vs. frequency plots for **1'$_{0.33}$**·CH_3OH in 1.4 kOe dc field with ac frequency of 0.1–1488 Hz. The lines are a guide for the eye.

Fig. S21 Dc field dependence of (a) the in-phase χ'_M vs. frequency plots and (b) out-of-phase χ''_M vs. frequency plots for **1'$_{0.33}$**·CH_3OH with ac frequency of 1–1488 Hz at 5.5 K. The lines are a guide for the eye.

Fig. S22 Temperature dependence of (a) the in-phase χ'_M vs. frequency plots and (b) out-of-phase χ''_M vs. frequency plots for **1'$_{0.12}$**·CH_3OH in 0 kOe dc field with ac frequency of 1–1488 Hz (1.9 K–2.6 K). The lines are a guide for the eye.

Fig. S23 Temperature dependence of (a) the in-phase χ'_M vs. frequency plots and (b) out-of-phase χ''_M vs. frequency plots for **1'$_{0.12}$**·CH_3OH in 1.4 kOe dc field with ac frequency of 0.1–1488 Hz. The lines are a guide for the eye.

Fig. S24 Dc field dependence of (a) the in-phase χ'_M vs. frequency plots and (b) out-of-phase χ''_M vs. frequency plots for **1'$_{0.12}$**·CH_3OH with ac frequency of 1–1488 Hz at 5.5 K. The lines are a guide for the eye.

Fig. S25 Cole-Cole plot for (a) **1'$_{0.33}$**·CH_3OH and (b) **1'$_{0.12}$**·CH_3OH in 1.4 kOe dc field from 1.9 to 8 K. The solid lines represent the fit to a generalized Debye model.

Table S16 Cole-Cole fit values for **1'$_{0.33}$**·CH_3OH in 1.4 kOe dc field from 1.9 to 7.5 K.

Table S17 Cole-Cole fit values for **1'$_{0.12}$**·CH_3OH in 1.4 kOe dc field from 1.9 to 8.0 K.

Fig. S26 Temperature dependence of (a) the in-phase χ'_M vs. frequency plots and (b) out-of-phase χ''_M vs. frequency plots for **2'$_{0.52}$** in 0 kOe dc field with ac frequency of 0.03–1488 Hz (1.9 K–8.0 K). The lines are a guide for the eye.

Fig. S27 Cole-Cole plot for **2'$_{0.52}$** in zero field from 1.9 to 8 K. The solid lines represent the fit to a generalized Debye model.

Table S18 Cole-Cole fit values for **2'$_{0.52}$** in zero dc field from 1.9 to 8.0 K.

Fig. S28 Temperature dependence of (a) the in-phase χ'_M vs. frequency plots and (b) out-of-phase χ''_M vs. frequency plots for **3'$_{0.67}$** in 0 kOe dc field with ac frequency of 0.03–1488 Hz (2.8 K–8.0 K). The lines are a guide for the eye.

Fig. S29 Cole-Cole plot for **3'$_{0.67}$** in zero field from 2.8 to 8 K. The solid lines represent the fit to a generalized Debye model.

Table S19 Cole-Cole fit values for **3'$_{0.67}$** in zero dc field from 2.8 to 8.0 K.

Fig. S30 Temperature dependence of the relaxation time τ for **1**·CH_3OH, **1'$_{0.33}$**·CH_3OH and **1'$_{0.12}$**·CH_3OH under 1.4 kOe dc field. The dashed lines indicate fitted lines for a single relaxation process of Raman $\tau^{-1} = CT^n$ and phonon-bottleneck limited direct process $\tau^{-1} = A_{pb}T^2$. The solid lines indicate the sum of the two relaxation processes.

Fig. 31 Field dependence of the relaxation time τ for **3** at 4.0 K. The dashed lines indicate fitted lines for a single relaxation process of QTM $\tau^{-1} = B_1/(1+B_2H^2)$, Raman $\tau^{-1} = CT^n$ and direct process $\tau^{-1} = ATH^4$. The solid lines indicate the sum of the two relaxation processes.

Table S20 Fitting parameters for the relaxation dynamics in **1**·CH_3OH, **1'$_{0.33}$**·CH_3OH and **1'$_{0.12}$**·CH_3OH.

Table S21 Fitting parameters for the relaxation dynamics in **2** and **2'$_{0.52}$**.

Table S22 Fitting parameters for the relaxation dynamics in **3** and **3'$_{0.67}$**.

Table S23 Fitting parameters for the relaxation dynamics in **4**·CH_3OH.

3. Powder X-ray diffraction measurement.

Fig. S32 Powder XRD patterns of **1**·CH_3OH, **1'$_{0.12}$**·CH_3OH, **1'$_{0.33}$**·CH_3OH and the simulated pattern of [Zn(Himl)$_2$]·CH_3OH at room temperature.

Fig. S33 Powder XRD patterns of **2**, and **2'$_{0.52}$** at room temperature, and the simulated pattern of [Zn(Himn)$_2$] at 90 K.

Fig. S34 Powder XRD patterns of **3** and **3'$_{0.67}$** at room temperature, and the simulated patterns of [Zn(Hthp)$_2$] at 90 K.

1. X-ray crystallography

Table S1. Crystallographic information.

Complex	**1**·CH_3OH	**2**	**3**	**4**·CH_3OH
Chemical formula	$C_{19}H_{18}CoN_4O_3$	$C_{18}H_{18}CoN_4O_2$	$C_{20}H_{22}CoN_4O_2$	$C_{21}H_{26}CoN_4O_5$
Formula weight	409.30	381.29	409.34	473.39
Color and shape of crystal	red, needle	red, prism	red, platelet	red, platelet
Size of specimen (mm^3)	0.36 × 0.12 × 0.12	0.45 × 0.20 × 0.20	0.30 × 0.30 × 0.20	0.14 × 0.12 × 0.06
Crystal system	orthorhombic	monoclinic	monoclinic	monoclinic
Space group	*Pbca*	$P2_1/n$	*C2/c*	$P2_1/c$
a / Å	9.6795(11)	11.9830(19)	13.789(3)	14.6617(18)
b / Å	14.4187(16)	7.6704(13)	11.399(3)	19.303(3)
c / Å	25.494(3)	18.692(3)	12.212(3)	7.5546(9)
β / °		105.227(2)	116.361(4)	104.276(3)
V / Å^3	3558.1(7)	1657.8(5)	1720.0(7)	2072.1(5)
Z	8	4	4	4
T / K	90(2)	90(2)	90(2)	90(2)
D_{calc}/ g cm^{-3}	1.528	1.528	1.581	1.517
F (000)	1688	788	852	988
μ(Mo-K$_a$) / mm^{-1}	0.993	1.055	1.023	0.870
R_{int}	0.0382	0.0378	0.0367	0.1195
$2\theta_{max}$/ °	57	57	57	55
No. of independent reflection	4417	3976	2101	4730
$R_1(F^2: F_o^2 > 2s\ (F_o^2))$	0.0363	0.0419	0.0403	0.0651
wR_2 (F^2: all data)	0.0946	0.1006	0.1231	0.1515

$R_1 = \Sigma||F_o|-|F_c||/\Sigma|F_o|$, $wR_2 = [\Sigma(F_o^2-F_c^2)/\Sigma w(F_o^2)^2]^{1/2}$

Table S2. Selected bond distances and angles of Co complexes (Å, °).

	1·CH_3OH	**2**	**3**	**4**·CH_3OH
Co–O	1.9220(13)	1.9389(16)	1.9184(17)	1.926(3)
	1.9309(13)	1.9357(16)		1.922(3)
Co–N	1.9776(15)	1.9593(18)	1.9551(19)	1.955(3)
	1.9566(16)	1.9586(18)		1.958(3)
O–Co–O	118.68(6)	109.91(7)	108.84(10)	115.35(13)
N–Co–N	126.70(6)	126.30(8)	125.99(11)	126.85(15)
O–Co–N (bite angle)	93.11(6)	93.56(7)	96.93(7)	93.60(14)
	94.67(6)	94.25(7)		93.63(14)
O–Co–N (inter ligand)	109.50(6)	113.33(7)	114.06(8)	108.20(13)
	116.15(6)	120.02(7)		120.18(14)

Table S3. Selected crystallographic information of the Zn analogues.

Complex	[Zn(Himl)$_2$]·CH$_3$OH [1]	[Zn(Himn)$_2$] [2]	[Zn(Hthp)$_2$] [3]
Chemical formula	$C_{19}H_{18}N_4O_3Zn$	$C_{18}H_{18}N_4O_2Zn$	$C_{20}H_{22}N_4O_2Zn$
Formula weight	415.74	387.73	415.78
Crystal system	orthorhombic	monoclinic	monoclinic
Space group	*Pbca*	$P2_1/n$	*C*2/*c*
a / Å	9.6943(19)	12.0318(15)	13.7667(14)
b / Å	14.77g(16)	7.6706(10)	11.4666(11)
c / Å	25.494(3)	18.617(2)	12.2213(12)
β / °		105.089(2)	116.242(2)
V / Å^3	3680.1(13)	1658.9(4)	1730.4(3)
Z	8	4	4
T / K	293(2)	90(2)	90(2)
D_{calc}/ g cm^{-3}	1.501	1.552	1.596
CCDC number	627785	1882004	1893923

Table S4. Selected bond distances, angles, and dihedral angles of Zn Complexes (Å, °).

	[Zn(Himl)$_2$]·CH$_3$OH [1]	[Zn(Himn)$_2$] [2]	[Zn(Hthp)$_2$] [3]
Zn1–O1	1.926(6)	1.952(2)	1.9229(16)
Zn1–O2	1.937(6)	1.9366(19)	
Zn1–N2	1.950(7)	1.951(2)	1.9526(19)
Zn1–N4	1.928(7)	1.952(2)	
O1–Zn1–O2(O1^{i})	113.9(3)	107.72(8)	106.98(10)
N2–Zn1–N4(N2^{i})	128.2(3)	127.66(10)	124.53(11)
O1–Zn1–N2	94.0(3)	94.61(9)	98.48(7)
O1–Zn1–N4(N2^{i})	115.1(3)	118.36(9)	113.97(7)
O2–Zn1–N2	110.9(3)	112.84(9)	
O2–Zn1–N4	95.8(3)	95.37(9)	

Symmetry code: (i = '–x+1, y, –z+3/2')

Table S5 Intrachain and the shortest interchain M···M distances (Å).

	Intrachain			Interchain		
2	Co1	Co1^{i}	6.048(1)	Co1	Co1^{iii}	7.6704(13)
	Co1	Co1^{ii}	6.254(1)			
[Zn(Himn)$_2$]	Zn1	Zn1^{i}	6.103(1)	Zn1	Zn1^{iii}	7.671(1)
	Zn1	Zn^{ii}	6.298(1)			
3	Co1	Co1^{i}	6.359(2)	Co1	Co1^{iv}	7.927(2)
[Zn(Hthp)$_2$]	Zn1	Zn1^{i}	6.372(1)	Zn1	Zn1^{iv}	7.934(1)
4	Co1	Co1^{i}	6.115(1)	Co1	Co1^{vi}	7.5546(9)
	Co1	Co1^{v}	8.680(1)			

Symmetry code: (i = '–x+1, –y+1, –z+1', ii = '–x, –y+1, –z+1', iii = 'x, y+1, z', iv = '–x+3/2, y+1/2, –z+3/2', v = '–x, –y, –z', vi = 'x, y, z+1').

1 H.-S. He, *Acta Crystallogr. Sect. E Struct. Reports Online*, 2006, **62**, m3042–m3043.
2 R. Mitsuhashi and M. Mikuriya, *X-ray Struct. Anal. Online*, 2019, **35**, 15–16.
3 R. Mitsuhashi and M. Mikuriya, *X-ray Struct. Anal. Online*, 2019, **35**, 37–38.

Table S6 Hydrogen-bond distances (Å) and angles (°).

	D	H	A	D–H	H···A	D···A	D–H···A
1·CH_3OH	N1	H1	$O2^{i}$	0.86(3)	1.95(3)	2.766(2)	156(2)
	O3	H3M	O1	0.84	1.81	2.6483(19)	171.7
	N3	H3A	$O3^{ii}$	0.83(3)	1.94(3)	2.752(2)	164(2)
[Zn(Himl)$_2$]·CH_3OH**Error! Bookmark not defined.**	N1	H1	$O2^{i}$	0.81(10)	2.01(10)	2.770(10)	157(10)
	O3	H3M	O1	0.82	1.88	2.653(10)	157
	N3	H3A	$O3^{ii}$	0.75(9)	2.09(10)	2.771(11)	152(11)
2	N1	H1	$O2^{iii}$	0.84(3)	2.03(3)	2.845(3)	164(3)
	N3	H3A	$O1^{ii}$	0.83(3)	2.03(3)	2.844(2)	165(2)
[Zn(Himn)$_2$]**Error! Bookmark not defined.**	N1	H1	$O2^{iv}$	0.75(3)	2.12(3)	2.832(2)	158(3)
	N3	H3A	$O1^{ii}$	0.85(3)	2.00(3)	2.828(3)	167(3)
3	N1	H1N	$O1^{v}$	0.81(3)	2.29(3)	3.059(3)	158(3)
[Zn(Hthp)$_2$]**Error! Bookmark not defined.**	N1	H1N	$O1^{vi}$	0.88(4)	2.20(4)	3.035(3)	157(3)
4·CH_3OH	N1	H1	$O5^{iii}$	0.85(4)	2.03(4)	2.853(5)	162(4)
	N3	H3N	$O1^{iii}$	0.795(19)	2.25(4)	2.927(5)	143(5)
	O5	H5A	O3	0.84	1.95	2.758(4)	161.3
	O5	H5A	O4	0.84	2.47	2.943(4)	116.4

Symmetry code: (i = 'x–1/2, y, –z+3/2 '; ii = '1–x, 1–y, 1–z'; iii = '–x, –y+1, –z+1'; iv = '2–x, 1–y, 1–z' v = 'x, –y+1, z–1/2 '; vi = 'x, –y+1, z+1/2 ').

2. Magnetic measurements.

Magnetic susceptibility measurements were performed with a MPMS-XL7 or MPMS-7 SQUID magnetometer. Susceptibility data were obtained in the temperature range from 1.9 to 300 K with static field of 0.5 T. The polycrystalline samples were ground into fine powders by an agate mortar. The samples were loaded into a gelatin capsule and covered in liquid paraffin to prevent field-induced orientation of crystals. All data were corrected for diamagnetism of the sample by means of Pascal's constants. The dynamic susceptibility was measured with alternating-current (ac) fields of 3 Oe magnitude and a constant direct current (dc) field of 0–5000 Oe in the frequency range from 0.03 to 1500 Hz.

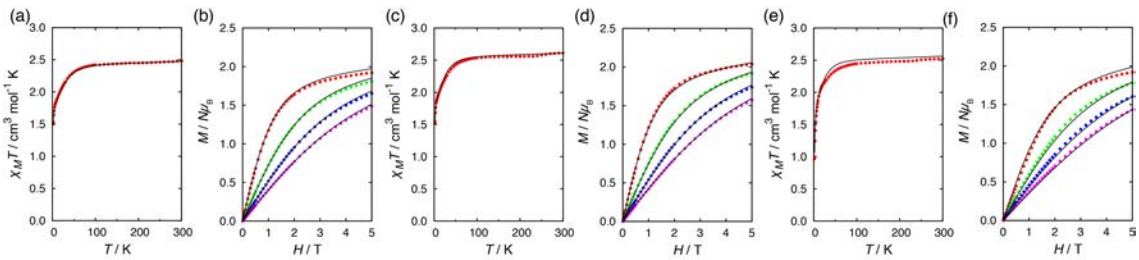

Fig. S1 Temperature dependence of the $\chi_M T$ product for (a) **1**·CH_3OH, (c) **2** and (e) **3** in an applied field of 5.0 kOe. Field dependence of the magnetization for (b) **1**·CH_3OH, (d) **2** and (f) **3** at 2, 4, 6 and 8 K (red green blue and magenta points, respectively).

Ac susceptibility measurements for **1**·CH_3OH

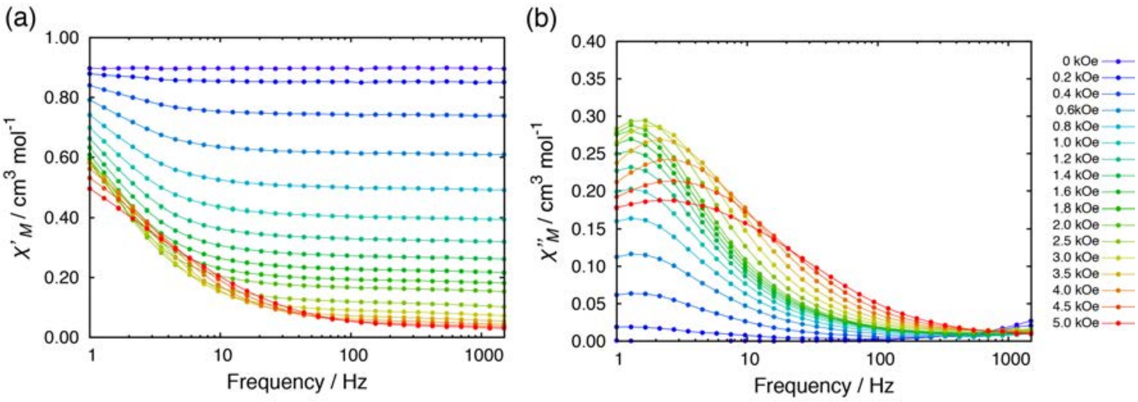

Fig. S2 Dc field dependence of (a) the in-phase χ'_M vs. frequency plots and (b) out-of-phase χ''_M vs. frequency plots for **1**·CH_3OH at 1.9 K with ac frequency of 0.1–1488 Hz. The lines are a guide for the eye.

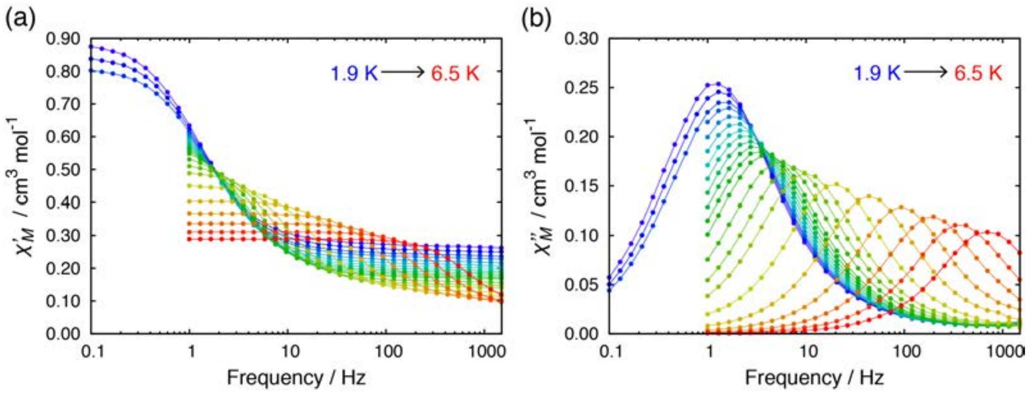

Fig. S3 Temperature dependence of (a) the in-phase χ'_M vs. frequency plots and (b) out-of-phase χ''_M vs. frequency plots for **1**·CH_3OH in 1.4 kOe dc field with ac frequency of 0.1–1488 Hz. The lines are a guide for the eye.

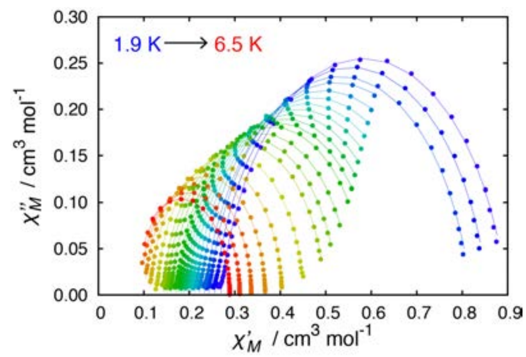

Fig. S4 Cole-Cole plot for **1**·CH_3OH in 1.4 kOe dc field from 1.9 to 6.5 K. The solid lines represent the fit to a generalized Debye model.

Table S7 Cole-Cole fit values for **1**·CH_3OH in 1.4 kOe dc field from 1.9 to 6.5 K.

T / K	χ_S / cm^3 mol^{-1}	χ_T / cm^3 mol^{-1}	τ / s	α
1.9	0.2689	0.8975	1.26×10^{-1}	0.132
2.0	0.2553	0.8573	1.15×10^{-1}	0.129
2.1	0.2425	0.8188	1.05×10^{-1}	0.126
2.2	0.2324	0.8103	1.03×10^{-1}	0.146
2.3	0.2211	0.7721	9.16×10^{-2}	0.140
2.4	0.2115	0.7387	8.22×10^{-2}	0.135
2.5	0.2029	0.7093	7.35×10^{-2}	0.129
2.6	0.1950	0.6836	6.59×10^{-2}	0.125
2.7	0.1879	0.6591	5.86×10^{-2}	0.120
2.8	0.1815	0.6357	5.19×10^{-2}	0.113
2.9	0.1751	0.6151	4.56×10^{-2}	0.108
3.0	0.1696	0.5948	3.98×10^{-2}	0.101
3.2	0.1591	0.5585	2.97×10^{-2}	0.087
3.4	0.1501	0.5262	2.17×10^{-2}	0.073
3.6	0.1422	0.4983	1.57×10^{-2}	0.061
4.0	0.1285	0.4517	8.08×10^{-3}	0.043
4.5	0.1145	0.4044	3.57×10^{-3}	0.029
5.0	0.1029	0.3673	1.67×10^{-3}	0.022
5.5	0.0922	0.3368	8.21×10^{-4}	0.021
6.0	0.0848	0.3111	4.29×10^{-4}	0.014
6.5	0.0755	0.2892	2.26×10^{-4}	0.016

Ac susceptibility measurements for **2**.

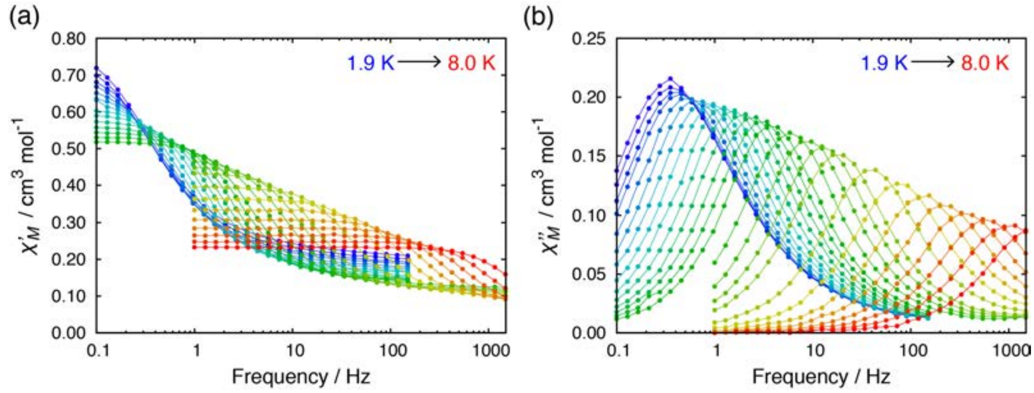

Fig. S5 Temperature dependence of (a) the in-phase χ'_M vs. frequency plots and (b) out-of-phase χ''_M vs. frequency plots for **2** in 0 Oe dc field with ac frequency of 0.1–1488 Hz (1.9 K–8.0 K). The lines are a guide for the eye.

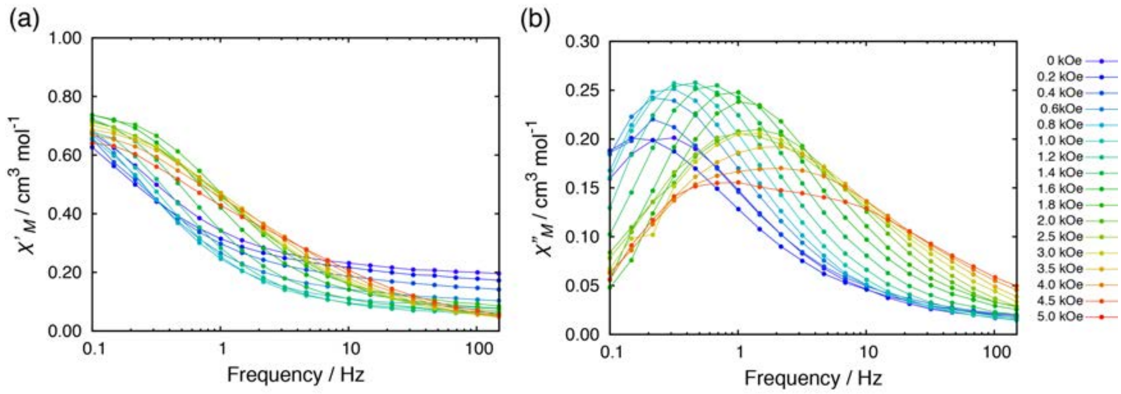

Fig. S6 Dc field dependence of (a) the in-phase χ'_M vs. frequency plots and (b) out-of-phase χ''_M vs. frequency plots for **2** with ac frequency of 0.1–148.8 Hz at 1.9 K. The lines are a guide for the eye.

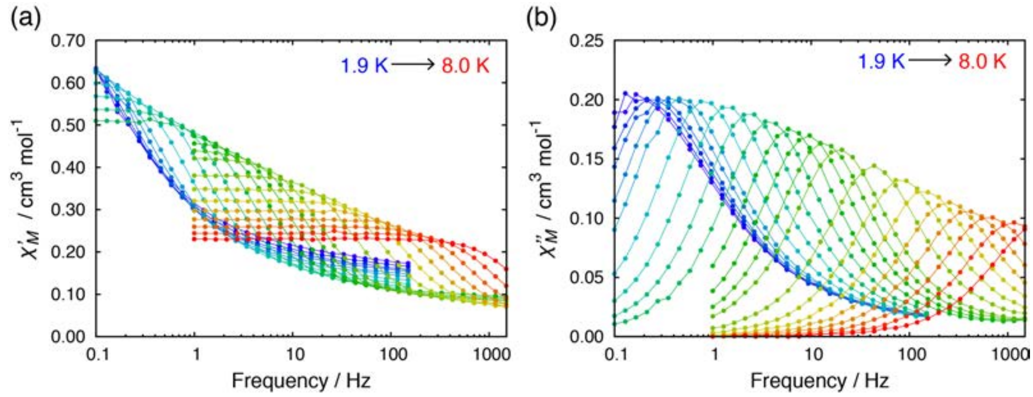

Fig. S7 Temperature dependence of (a) the in-phase χ'_M vs. frequency plots and (b) out-of-phase χ''_M vs. frequency plots for **2** in 0.4 kOe dc field with ac frequency of 0.1–1488 Hz (1.9 K–8.0 K). The lines are a guide for the eye. The lines are a guide for the eye.

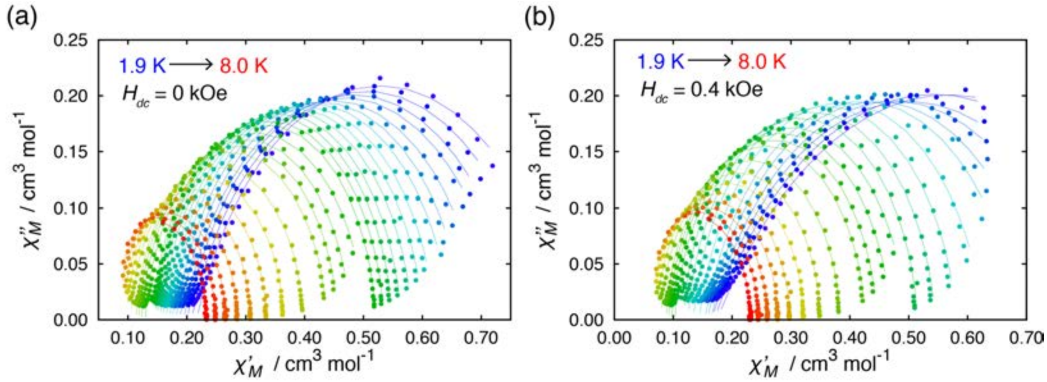

Fig. S8 Cole-Cole plot for **2** (a) in zero field and (b) in 0.4 kOe dc field from 1.9 to 8 K. The solid lines represent the fit to a generalized Debye model.

Table S8 Cole-Cole fit values for **2** in zero dc field from 1.9 to 8.0 K.

T / K	χ_S / cm$_3$ mol^{-1}	χ_T / cm$_3$ mol^{-1}	τ / s	α
1.9	0.2166	0.8411	4.45×10^{-1}	0.249
2.0	0.2078	0.8027	4.08×10^{-1}	0.235
2.1	0.2003	0.7659	3.63×10^{-1}	0.213
2.2	0.1948	0.7407	3.30×10^{-1}	0.200
2.3	0.1876	0.7028	2.74×10^{-1}	0.172
2.4	0.1816	0.6732	2.29×10^{-1}	0.148
2.5	0.1751	0.6493	1.89×10^{-1}	0.131
2.6	0.1707	0.6224	1.52×10^{-1}	0.107
2.7	0.1650	0.6021	1.22×10^{-1}	0.094
2.8	0.1591	0.5829	9.76×10^{-2}	0.081
2.9	0.1543	0.5640	7.79×10^{-2}	0.069
3.0	0.1499	0.5486	6.24×10^{-2}	0.061
3.1	0.1466	0.5348	5.00×10^{-2}	0.057
3.2	0.1430	0.5209	4.01×10^{-2}	0.051
3.4	0.1296	0.5023	2.65×10^{-2}	0.070
3.6	0.1234	0.4771	1.76×10^{-2}	0.060
3.8	0.1184	0.4561	1.21×10^{-2}	0.053
4.0	0.1141	0.4373	8.49×10^{-3}	0.049
4.5	0.1048	0.3978	3.92×10^{-3}	0.044
5.0	0.0976	0.3641	2.04×10^{-3}	0.038
5.5	0.0911	0.3351	1.16×10^{-3}	0.030
6.0	0.0833	0.3081	7.04×10^{-4}	0.026
6.5	0.0771	0.2853	4.41×10^{-4}	0.016
7.0	0.0686	0.2654	2.70×10^{-4}	0.017
7.5	0.0605	0.2485	1.60×10^{-4}	0.015
8.0	0.0522	0.2331	8.92×10^{-5}	0.010

Table S9 Cole-Cole fit values for **2** in 0.4 kOe dc field from 1.9 to 8.0 K.

T / K	χ_S / cm3 mol^{-1}	χ_T / cm3 mol^{-1}	τ / s	α
1.9	0.1747	0.9610	1.17×10^{0}	0.399
2.0	0.1693	0.9159	9.68×10^{-1}	0.370
2.1	0.1650	0.8352	7.04×10^{-1}	0.330
2.2	0.1631	0.7879	5.48×10^{-1}	0.289
2.3	0.1579	0.7319	3.98×10^{-1}	0.240
2.4	0.1537	0.6897	3.00×10^{-1}	0.199
2.6	0.1441	0.6269	1.75×10^{-1}	0.138
2.8	0.1343	0.5812	1.04×10^{-1}	0.100
3.0	0.1254	0.5447	6.31×10^{-2}	0.077
3.2	0.1172	0.5149	3.94×10^{-2}	0.062
3.4	0.1026	0.4968	2.54×10^{-2}	0.087
3.6	0.0972	0.4693	1.66×10^{-2}	0.070
3.8	0.0923	0.4465	1.13×10^{-2}	0.062
4.0	0.0881	0.4264	7.85×10^{-3}	0.054
4.5	0.0795	0.3834	3.56×10^{-3}	0.042
5.0	0.0718	0.3500	1.83×10^{-3}	0.036
5.5	0.0658	0.3220	1.04×10^{-3}	0.032
6.0	0.0599	0.2982	6.23×10^{-4}	0.034
6.5	0.0561	0.2779	3.91×10^{-4}	0.027
7.0	0.0509	0.2601	2.40×10^{-4}	0.024
7.5	0.0459	0.2446	1.43×10^{-4}	0.020
8.0	0.0395	0.2311	8.15×10^{-5}	0.017

Ac susceptibility measurements for **3**.

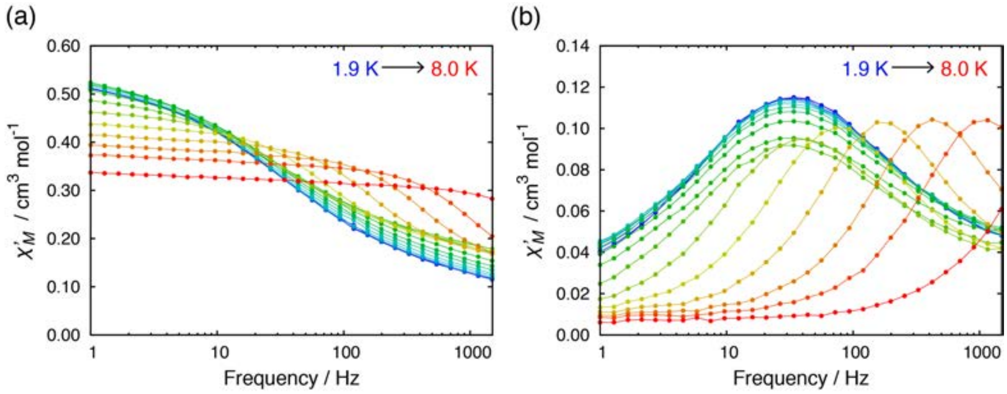

Fig. S9 Temperature dependence of (a) the in-phase χ'_M vs. frequency plots and (b) out-of-phase χ''_M vs. frequency plots for **3** in 0 Oe dc field with ac frequency of 1–1488 Hz (1.9 K–8.0 K). The lines are a guide for the eye.

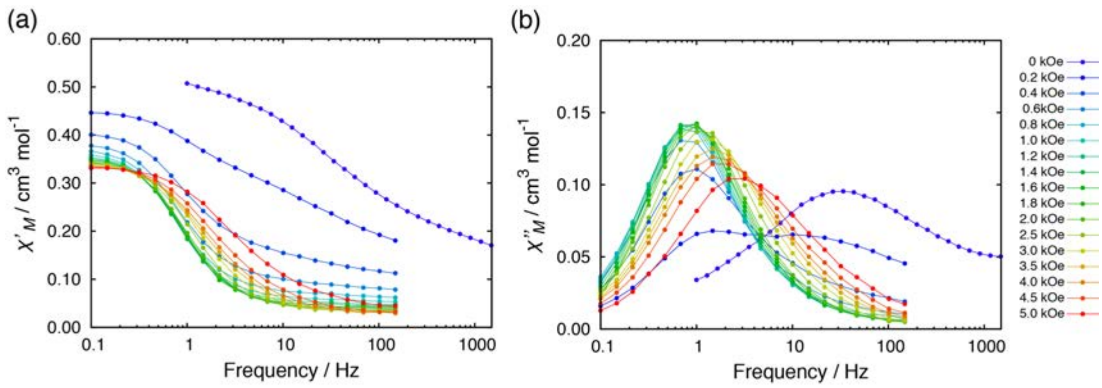

Fig. S10 Dc field dependence of (a) the in-phase χ'_M vs. frequency plots and (b) out-of-phase χ''_M vs. frequency plots for **3** with ac frequency of 0.1–1488 Hz at 4 K. The lines are a guide for the eye.

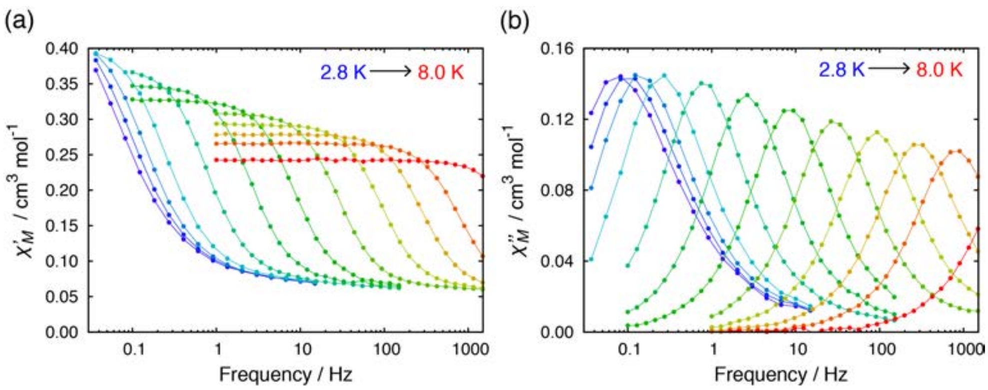

Fig. S11 Temperature dependence of (a) the in-phase χ'_M vs. frequency plots and (b) out-of-phase χ''_M vs. frequency plots for **3** in 0.8 kOe dc field with ac frequency of 0.03–1488 Hz (2.8 K–8.0 K). The lines are a guide for the eye.

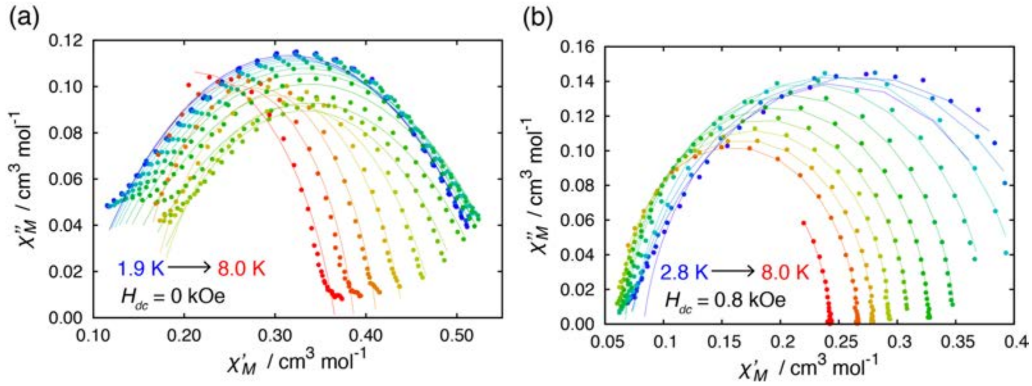

Fig. S12 Cole-Cole plot for **3** (a) in zero field and (b) in 0.8 kOe dc field from 1.9 to 8 K. The solid lines represent the fit to a generalized Debye model.

Table S10 Cole-Cole fit values for **3** in zero dc field from 1.9 to 8.0 K.

T / K	χ_S / cm3 mol^{-1}	χ_T / cm3 mol^{-1}	τ / s	α
1.9	0.0820	0.5495	4.15×10^{-3}	0.424
2.0	0.0820	0.5485	4.20×10^{-3}	0.423
2.2	0.0813	0.5506	4.27×10^{-3}	0.430
2.4	0.0823	0.5554	4.37×10^{-3}	0.437
2.6	0.0848	0.5611	4.44×10^{-3}	0.444
2.8	0.0871	0.5671	4.39×10^{-3}	0.454
3.0	0.0928	0.5704	4.31×10^{-3}	0.459
3.2	0.0995	0.5700	4.21×10^{-3}	0.462
3.5	0.1114	0.5645	4.05×10^{-3}	0.465
4.0	0.1306	0.5466	3.95×10^{-3}	0.465
4.5	0.1517	0.5157	3.86×10^{-3}	0.418
5.0	0.1625	0.4777	3.06×10^{-3}	0.328
5.5	0.1592	0.4416	1.80×10^{-3}	0.237
6.0	0.1453	0.4118	8.46×10^{-4}	0.183
6.5	0.1196	0.3868	3.43×10^{-4}	0.176
7.0	0.0538	0.3659	1.05×10^{-4}	0.238
8.0	0.0000	0.3301	1.12×10^{-5}	0.400

Table S11 Cole-Cole fit values for **3** in 0.8 kOe dc field from 2.8 to 8.0 K.

T / K	χ_S / cm3 mol^{-1}	χ_T / cm3 mol^{-1}	τ / s	α
2.8	0.0830	0.4132	1.40×10^{0}	0.110
3.0	0.0702	0.4666	1.51×10^{0}	0.205
3.2	0.0712	0.4420	1.06×10^{0}	0.161
3.5	0.0733	0.4093	5.80×10^{-1}	0.099
4.0	0.0671	0.3785	1.93×10^{-1}	0.074
4.5	0.0669	0.3495	5.92×10^{-2}	0.043
5.0	0.0653	0.3278	1.82×10^{-2}	0.032
5.5	0.0618	0.3101	5.43×10^{-3}	0.033
6.0	0.0609	0.2938	1.68×10^{-3}	0.027

6.5	0.0583	0.2793	5.50×10^{-4}	0.026
7.0	0.0532	0.2661	1.96×10^{-4}	0.026
8.0	0.0317	0.2426	3.22×10^{-5}	0.038

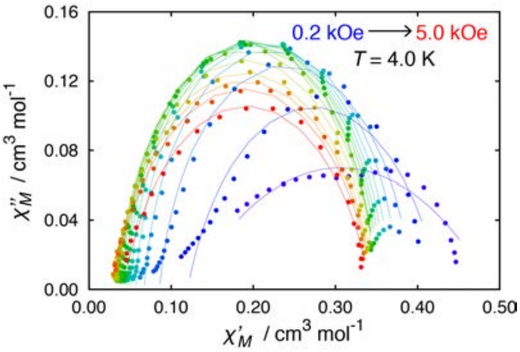

Fig. S13 Cole-Cole plot for **3** under 0.2–5.0 kOe. The solid lines represent the fit to a generalized Debye model.

Table S12 Cole-Cole fit values for **3** at 4 K with an applied dc field of 0.2 to 5.0 kOe.

H_{dc} / kOe	χ_S / cm3 mol^{-1}	χ_T / cm3 mol^{-1}	τ / s	α
0.2	0.1228	0.4895	2.48×10^{-2}	0.54
0.4	0.1200	0.4271	1.40×10^{-1}	0.24
0.6	0.0859	0.3930	1.82×10^{-1}	0.11
0.8	0.0674	0.3774	1.92×10^{-1}	0.07
1.0	0.0570	0.3673	1.90×10^{-1}	0.06
1.2	0.0505	0.3611	1.83×10^{-1}	0.05
1.4	0.0462	0.3567	1.76×10^{-1}	0.05
1.6	0.0434	0.3530	1.68×10^{-1}	0.05
1.8	0.0403	0.3497	1.59×10^{-1}	0.05
2.0	0.0379	0.3496	1.51×10^{-1}	0.06
2.5	0.0341	0.3501	1.30×10^{-1}	0.08
3.0	0.0329	0.3486	1.10×10^{-1}	0.11
3.5	0.0297	0.3478	9.75×10^{-2}	0.15
4.0	0.0291	0.3474	8.82×10^{-2}	0.18
4.5	0.0303	0.3466	7.30×10^{-2}	0.20
5.0	0.0411	0.3431	4.85×10^{-2}	0.22

Ac susceptibility measurements for **4**·CH_3OH.

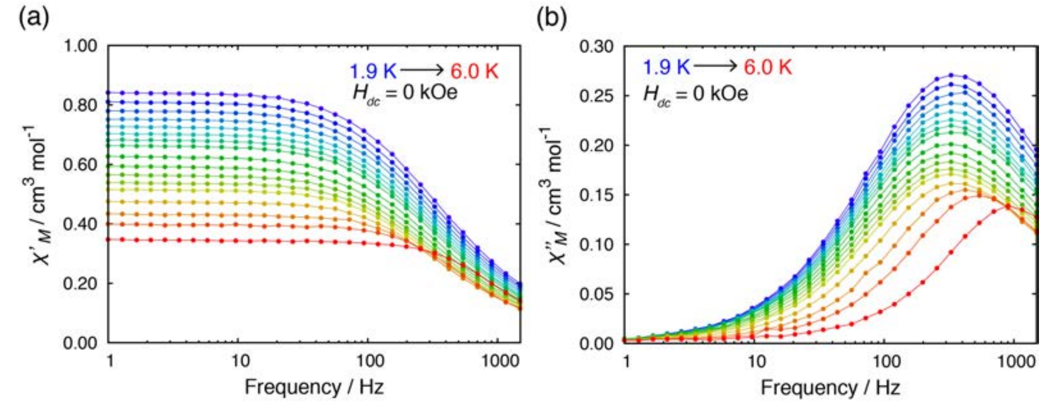

Fig. S14 Temperature dependence of (a) the in-phase χ'_M vs. frequency plots and (b) out-of-phase χ''_M vs. frequency plots for **4**·CH_3OH in 0 Oe dc field with ac frequency of 1–1488 Hz (1.9 K–6.0 K). The lines are a guide for the eye.

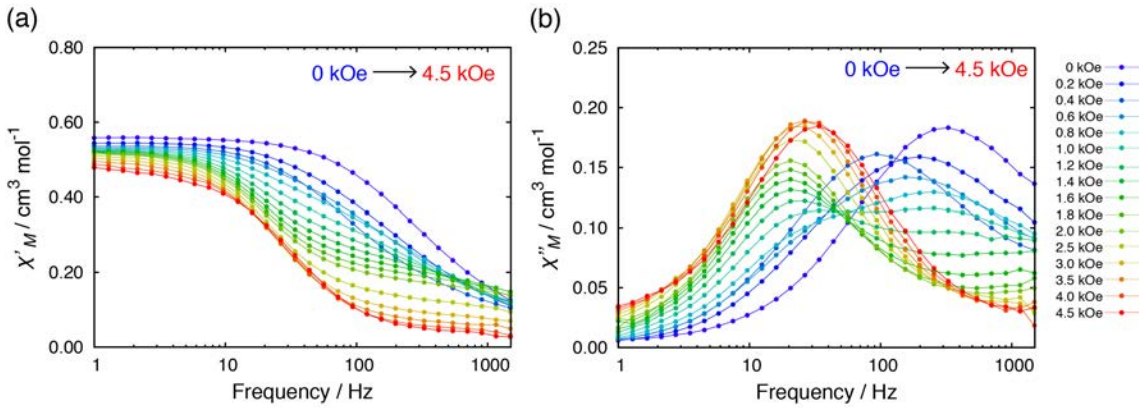

Fig. S15 Dc field dependence of (a) the in-phase χ'_M vs. frequency plots and (b) out-of-phase χ''_M vs. frequency plots for **4**·CH_3OH with ac frequency of 1–1488 Hz at 3.4 K. The lines are a guide for the eye.

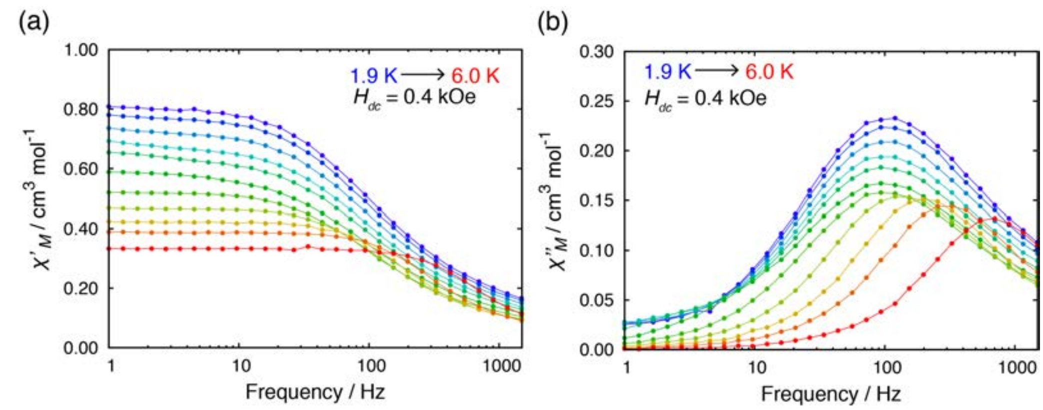

Fig. S16 Temperature dependence of (a) the in-phase χ'_M vs. frequency plots and (b) out-of-phase χ''_M vs. frequency plots for **4**·CH_3OH in 0.4 kOe dc field with ac frequency of 1–1488 Hz

(1.9 K–6.0 K). The lines are a guide for the eye.

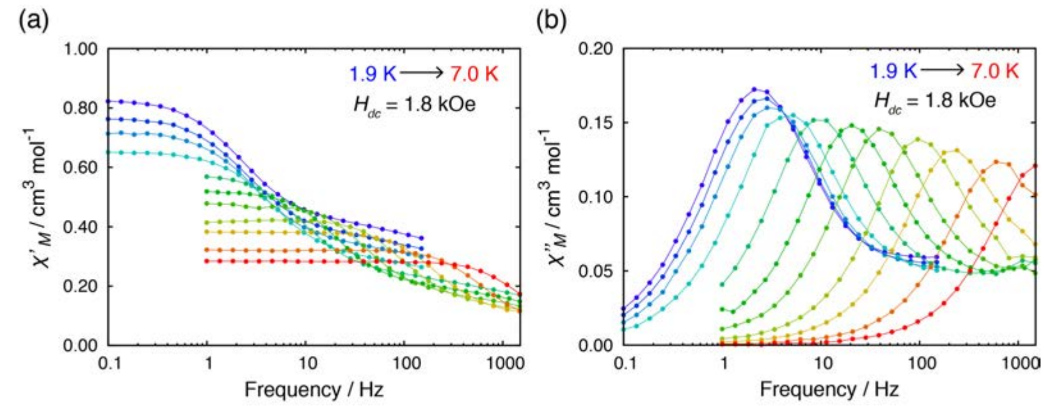

Fig. S17 Temperature dependence of (a) the in-phase χ'_M vs. frequency plots and (b) out-of-phase χ''_M vs. frequency plots for **4**·CH_3OH in 1.8 kOe dc field with ac frequency of 0.1–1488 Hz (1.9 K–7.0 K). The lines are a guide for the eye.

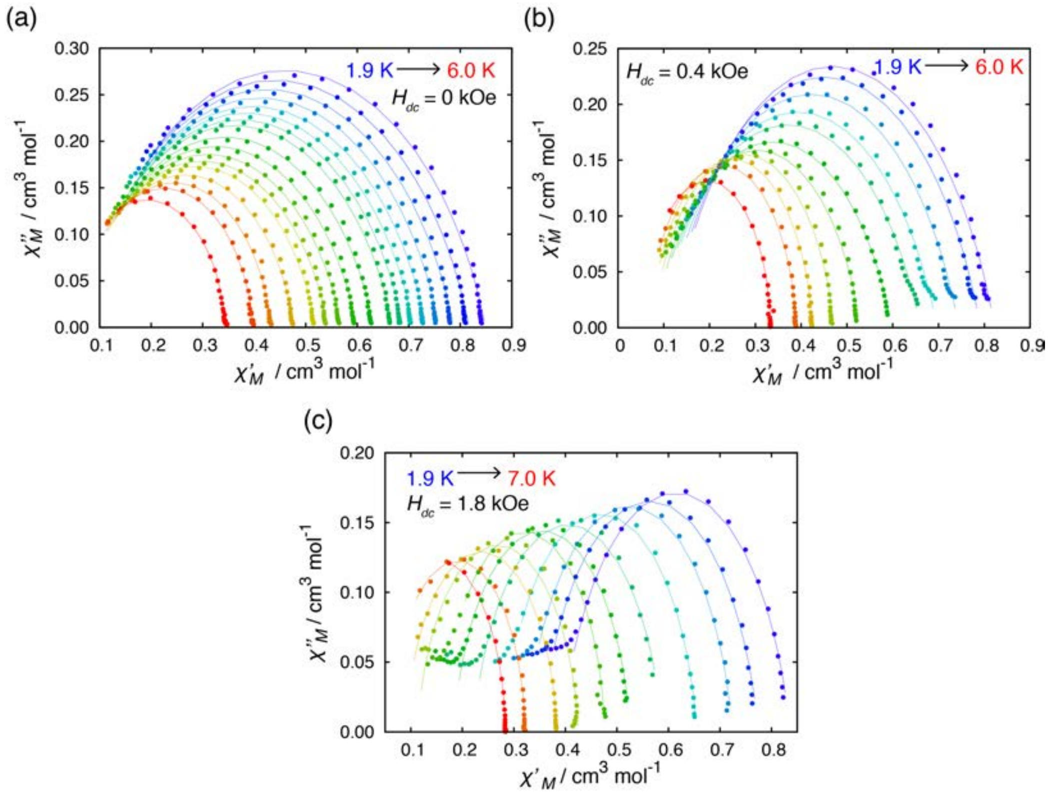

Fig. S18 Cole-Cole plot for **4**·CH_3OH (a) in zero field from 1.9 to 6 K, (b) in 0.4 kOe dc field from 1.9 to 6 K and (c) in 1.8 Oe dc field from 1.9 to 7 K. The solid lines represent the fit to a generalized Debye model.

Table S13 Cole-Cole fit values for **4**·CH_3OH in zero dc field from 1.9 to 6.0 K.

T / K	χ_S / cm_3 mol^{-1}	χ_T / cm_3 mol^{-1}	τ / s	α
1.9	0.0694	0.8491	4.40×10^{-4}	0.215
2.0	0.0652	0.8176	4.42×10^{-4}	0.217
2.1	0.0633	0.7876	4.47×10^{-4}	0.217
2.2	0.0651	0.7593	4.54×10^{-4}	0.213
2.3	0.0596	0.7342	4.53×10^{-4}	0.218
2.4	0.0582	0.7102	4.56×10^{-4}	0.216
2.5	0.0574	0.6893	4.60×10^{-4}	0.217
2.6	0.0551	0.6694	4.60×10^{-4}	0.216
2.8	0.0558	0.6322	4.68×10^{-4}	0.214
3.0	0.0533	0.5990	4.68×10^{-4}	0.211
3.2	0.0520	0.5695	4.65×10^{-4}	0.206
3.4	0.0533	0.5429	4.61×10^{-4}	0.197
3.6	0.0534	0.5190	4.51×10^{-4}	0.185
4.0	0.0549	0.4771	4.18×10^{-4}	0.159
4.5	0.0536	0.4335	3.52×10^{-4}	0.126
5.0	0.0519	0.3978	2.85×10^{-4}	0.091
6.0	0.0382	0.3443	1.64×10^{-4}	0.069

Table S14 Cole-Cole fit values for **4**·CH_3OH in 0.4 kOe dc field from 1.9 to 6.0 K.

T / K	χ_S / cm_3 mol^{-1}	χ_T / cm_3 mol^{-1}	τ / s	α
1.9	0.1150	0.8227	1.29×10^{-3}	0.256
2.0	0.1090	0.7917	1.30×10^{-3}	0.259
2.2	0.1003	0.7443	1.33×10^{-3}	0.267
2.4	0.0891	0.6968	1.36×10^{-3}	0.279
2.6	0.0826	0.6604	1.40×10^{-3}	0.285
3.0	0.0780	0.5989	1.45×10^{-3}	0.276
3.5	0.0798	0.5297	1.32×10^{-3}	0.216
4.0	0.0773	0.4720	1.03×10^{-3}	0.151
4.5	0.0725	0.4254	7.21×10^{-4}	0.098
5.0	0.0665	0.3893	4.94×10^{-4}	0.067
6.0	0.0560	0.3333	2.31×10^{-4}	0.032

Table S15 Cole-Cole fit values for **4**·CH_3OH in 1.8 kOe dc field from 1.9 to 7.0 K.

T / K	χ_S / cm_3 mol^{-1}	χ_T / cm_3 mol^{-1}	τ / s	α
1.9	0.3931	0.8358	6.50×10^{-2}	0.161
2.1	0.3532	0.7743	5.68×10^{-2}	0.152
2.3	0.3240	0.7242	4.82×10^{-2}	0.135
2.6	0.2813	0.6549	3.26×10^{-2}	0.113
3.0	0.2214	0.5883	1.53×10^{-2}	0.133
3.8	0.1637	0.4765	3.63×10^{-3}	0.054
4.4	0.1125	0.4258	1.35×10^{-3}	0.099
5.0	0.0897	0.3843	6.56×10^{-4}	0.083
6.0	0.0598	0.3220	2.38×10^{-4}	0.041
7.0	0.0228	0.2838	9.24×10^{-5}	0.034

i. Some data points in high field at low temperature region were removed from fitting to model with single Debye function.

Ac susceptibility measurements for Zn^{II}-doped samples: **1'$_{\mathbf{x}}$**$\cdot CH_3OH$.

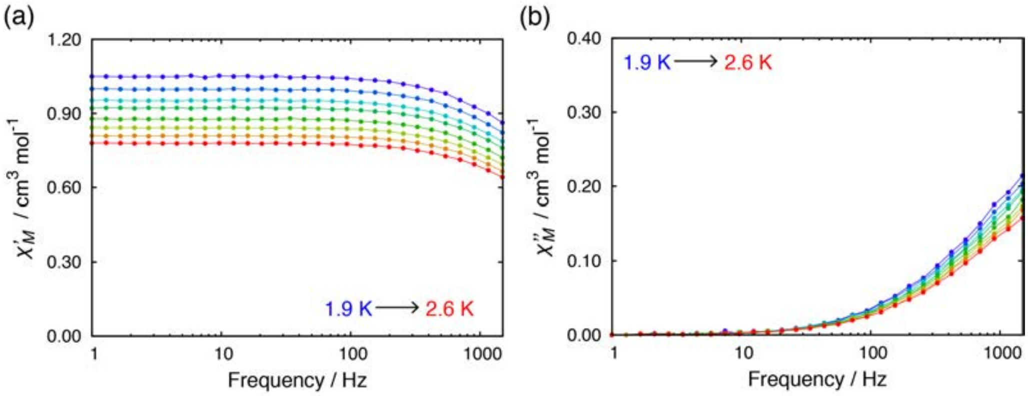

Fig. S19 Temperature dependence of (a) the in-phase χ'_M vs. frequency plots and (b) out-of-phase χ''_M vs. frequency plots for **1'$_{\mathbf{0.33}}$**$\cdot CH_3OH$ in 0 kOe dc field with ac frequency of 1–1488 Hz (1.9 K–2.6 K). The lines are a guide for the eye.

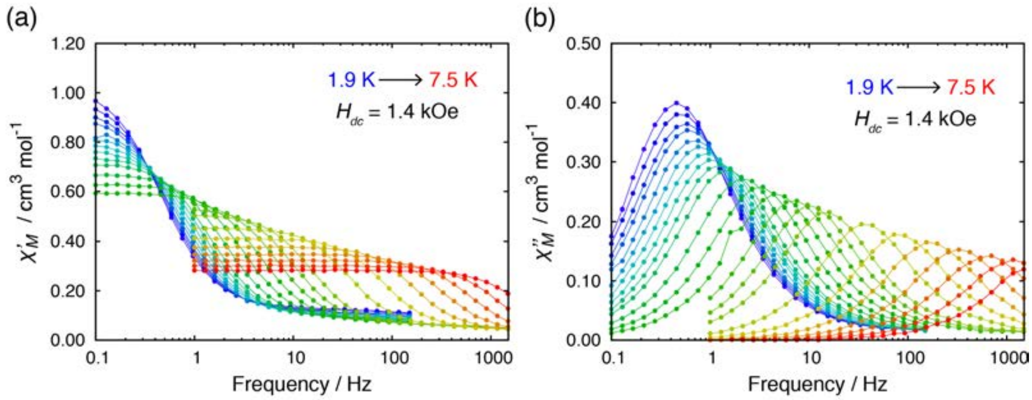

Fig. S20 Temperature dependence of (a) the in-phase χ'_M vs. frequency plots and (b) out-of-phase χ''_M vs. frequency plots for **1'$_{\mathbf{0.33}}$**$\cdot CH_3OH$ in 1.4 kOe dc field with ac frequency of 0.1–1488 Hz. The lines are a guide for the eye.

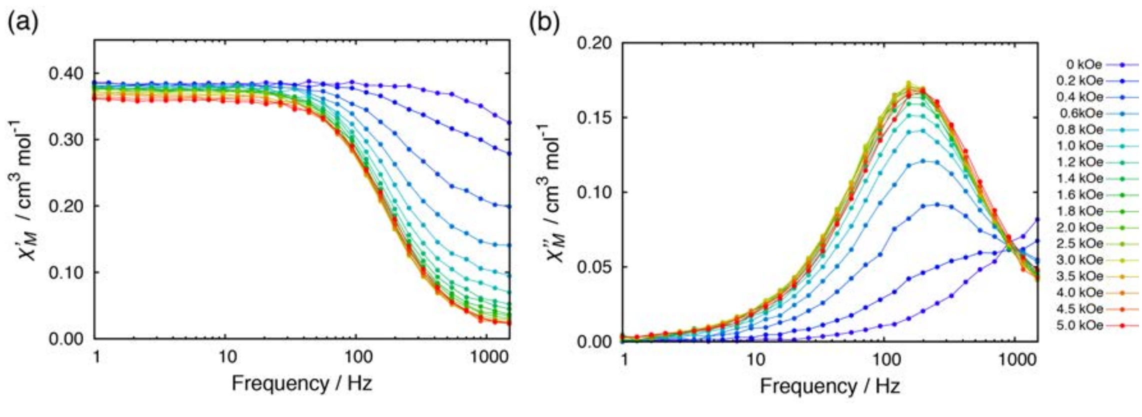

Fig. S21 Dc field dependence of (a) the in-phase χ'_M vs. frequency plots and (b) out-of-phase

χ''_M vs. frequency plots for **1'$_{0.33}$**·CH_3OH with ac frequency of 1–1488 Hz at 5.5 K. The lines are a guide for the eye.

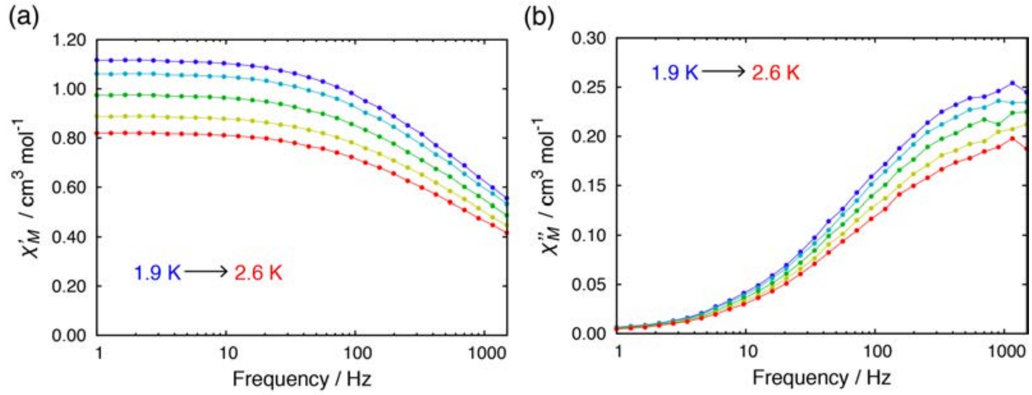

Fig. S22 Temperature dependence of (a) the in-phase χ'_M vs. frequency plots and (b) out-of-phase χ''_M vs. frequency plots for **1'$_{0.12}$**·CH_3OH in 0 kOe dc field with ac frequency of 1–1488 Hz (1.9 K–2.6 K). The lines are a guide for the eye.

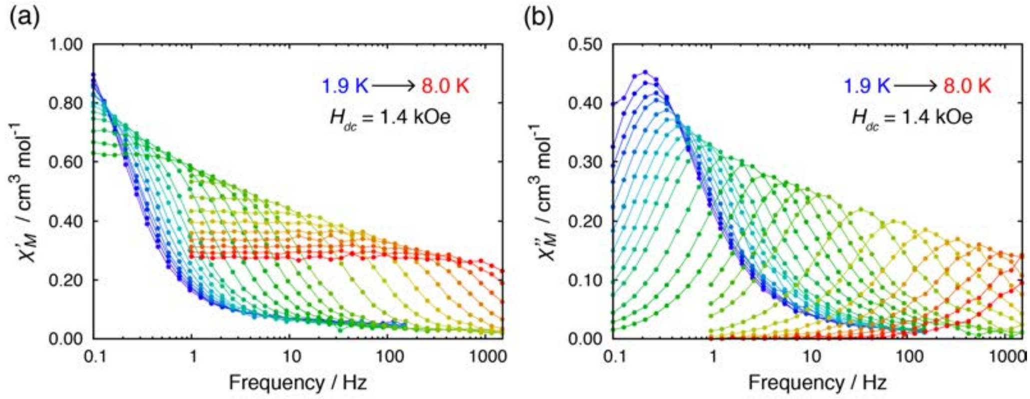

Fig. S23 Temperature dependence of (a) the in-phase χ'_M vs. frequency plots and (b) out-of-phase χ''_M vs. frequency plots for **1'$_{0.12}$**·CH_3OH in 1.4 kOe dc field with ac frequency of 0.1–1488 Hz. The lines are a guide for the eye.

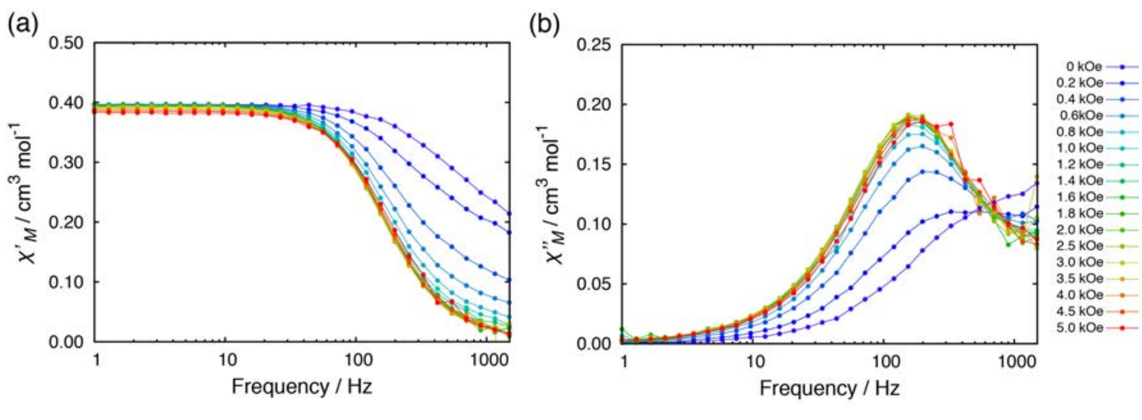

Fig. S24 Dc field dependence of (a) the in-phase χ'_M vs. frequency plots and (b) out-of-phase χ''_M vs. frequency plots for **1'$_{0.12}$**·CH_3OH with ac frequency of 1–1488 Hz at 5.5 K. The lines are a guide for the eye.

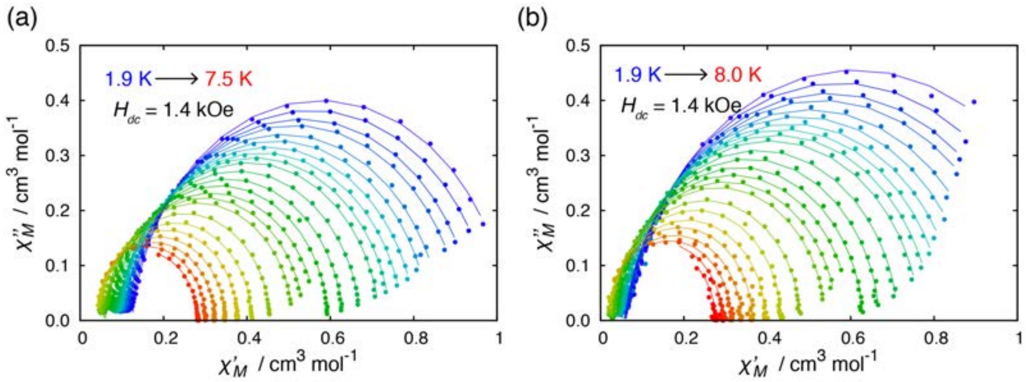

Fig. S25 Cole-Cole plot for (a) **1'$_{0.33}$**·CH_3OH and (b) **1'$_{0.12}$**·CH_3OH in 1.4 kOe dc field from 1.9 to 8 K. The solid lines represent the fit to a generalized Debye model.

Table S16 Cole-Cole fit values for **1'$_{0.33}$**·CH_3OH in 1.4 kOe dc field from 1.9 to 7.5 K.

T / K	χ_S / cm$_3$ mol^{-1}	χ_T / cm$_3$ mol^{-1}	τ / s	α
1.9	0.1244	1.0291	3.34×10^{-1}	0.078
2.0	0.1185	0.9909	3.06×10^{-1}	0.084
2.1	0.1130	0.9478	2.74×10^{-1}	0.083
2.2	0.1096	0.9175	2.53×10^{-1}	0.082
2.3	0.1049	0.8680	2.19×10^{-1}	0.076
2.4	0.1018	0.8385	1.94×10^{-1}	0.076
2.5	0.0965	0.8057	1.69×10^{-1}	0.074
2.6	0.0941	0.7755	1.45×10^{-1}	0.070
2.7	0.0917	0.7455	1.24×10^{-1}	0.063
2.8	0.0888	0.7190	1.05×10^{-1}	0.059
3.0	0.0832	0.6726	7.35×10^{-2}	0.051
3.2	0.0785	0.6306	4.98×10^{-2}	0.044
3.4	0.0732	0.5957	3.39×10^{-2}	0.040
3.6	0.0605	0.5686	2.24×10^{-2}	0.058
3.8	0.0576	0.5379	1.52×10^{-2}	0.047
4.0	0.0545	0.5109	1.03×10^{-2}	0.041
4.5	0.0480	0.4556	4.17×10^{-3}	0.029
5.0	0.0432	0.4124	1.88×10^{-3}	0.024
5.5	0.0392	0.3775	9.16×10^{-4}	0.017
6.0	0.0354	0.3475	4.74×10^{-4}	0.017
6.5	0.0305	0.3222	2.56×10^{-4}	0.016
7.0	0.0244	0.3008	1.40×10^{-4}	0.017
7.5	0.0238	0.2820	8.05×10^{-5}	0.016

Table S17 Cole-Cole fit values for **1'$_{0.12}$**·CH_3OH in 1.4 kOe dc field from 1.9 to 8.0 K.

T / K	χ_S / cm_3 mol^{-1}	χ_T / cm_3 mol^{-1}	τ / s	α
1.9	0.0613	1.1610	7.85×10^{-1}	0.119
2.0	0.0592	1.0874	6.78×10^{-1}	0.111
2.1	0.0572	1.0368	5.99×10^{-1}	0.108
2.2	0.0562	1.0045	5.45×10^{-1}	0.107
2.3	0.0561	0.9457	4.52×10^{-1}	0.094
2.4	0.0521	0.9014	3.78×10^{-1}	0.086
2.5	0.0509	0.8631	3.13×10^{-1}	0.081
2.6	0.0482	0.8299	2.54×10^{-1}	0.075
2.7	0.0480	0.7975	2.05×10^{-1}	0.067
2.8	0.0461	0.7680	1.64×10^{-1}	0.063
3.0	0.0428	0.7148	1.04×10^{-1}	0.052
3.2	0.0411	0.6695	6.56×10^{-2}	0.043
3.4	0.0382	0.6301	4.17×10^{-2}	0.039
3.6	0.0315	0.6007	2.69×10^{-2}	0.046
3.8	0.0290	0.5681	1.75×10^{-2}	0.042
4.0	0.0274	0.5401	1.16×10^{-2}	0.037
4.5	0.0243	0.4796	4.55×10^{-3}	0.026
5.0	0.0226	0.4332	2.01×10^{-3}	0.013
5.5	0.0210	0.3960	9.75×10^{-4}	0.016
6.0	0.0176	0.3642	4.98×10^{-4}	0.014
6.5	0.0177	0.3382	2.71×10^{-4}	0.020
7.0	0.0186	0.3137	1.48×10^{-4}	0.010
7.5	0.0000	0.2936	7.84×10^{-5}	0.024
8.0	0.0000	0.2766	4.51×10^{-5}	0.022

Ac susceptibility measurements for Zn^{II}-doped samples: **2'$_{0.52}$**.

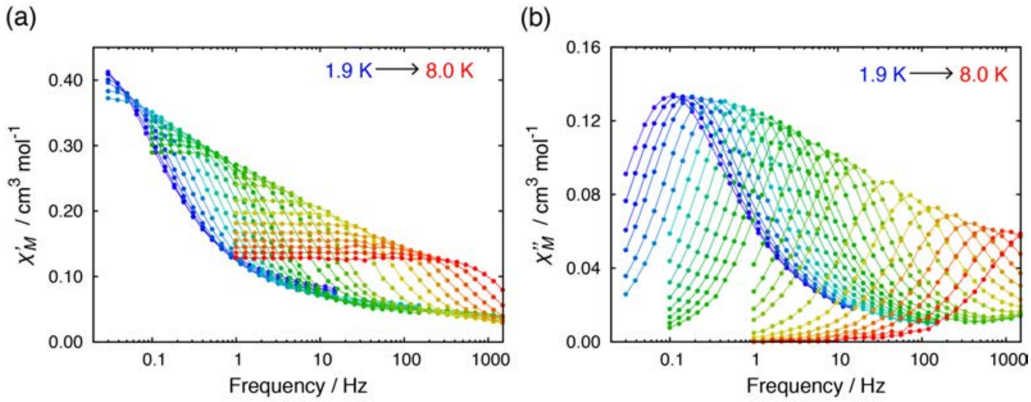

Fig. S26 Temperature dependence of (a) the in-phase χ'_M vs. frequency plots and (b) out-of-phase χ''_M vs. frequency plots for **2'$_{0.52}$** in 0 kOe dc field with ac frequency of 0.03–1488 Hz (1.9 K–8.0 K). The lines are a guide for the eye.

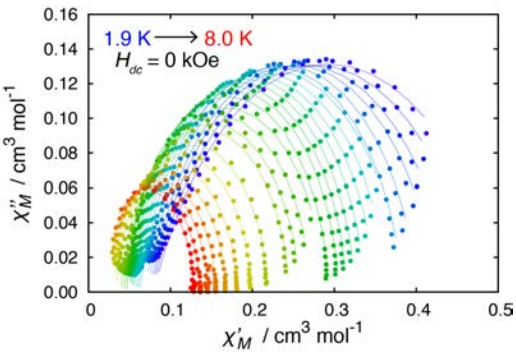

Fig. S27 Cole-Cole plot for **2'$_{0.52}$** in zero field from 1.9 to 8 K. The solid lines represent the fit to a generalized Debye model.

Table S18 Cole-Cole fit values for **2'$_{0.52}$** in zero dc field from 1.9 to 8.0 K.

T / K	χ_S / cm3 mol^{-1}	χ_T / cm3 mol^{-1}	τ / s	α
1.9	0.1546	0.9800	1.45×10^{0}	0.296
2.0	0.1521	0.9193	1.17×10^{0}	0.256
2.1	0.1496	0.8634	9.08×10^{-1}	0.213
2.2	0.1464	0.8276	7.49×10^{-1}	0.185
2.3	0.1416	0.7811	5.50×10^{-1}	0.147
2.4	0.1365	0.7454	4.14×10^{-1}	0.120
2.6	0.1164	0.7097	2.35×10^{-1}	0.122
2.7	0.1131	0.6810	1.78×10^{-1}	0.103
2.8	0.1082	0.6551	1.33×10^{-1}	0.088
2.9	0.1049	0.6317	1.01×10^{-1}	0.076
3.0	0.1012	0.6114	7.81×10^{-2}	0.069
3.1	0.0976	0.5924	6.07×10^{-2}	0.061
3.2	0.0911	0.5688	4.75×10^{-2}	0.055
3.4	0.0908	0.5588	3.05×10^{-2}	0.081

3.6	0.0857	0.5262	1.97×10^{-2}	0.069
3.8	0.0806	0.4995	1.32×10^{-2}	0.068
4.0	0.0764	0.4747	9.11×10^{-3}	0.060
4.5	0.0663	0.4246	4.03×10^{-3}	0.055
5.0	0.0589	0.3851	2.07×10^{-3}	0.046
5.5	0.0502	0.3527	1.15×10^{-3}	0.050
6.0	0.0443	0.3250	6.86×10^{-4}	0.044
6.5	0.0376	0.3015	4.21×10^{-4}	0.040
7.0	0.0307	0.2821	2.57×10^{-4}	0.035
7.5	0.0234	0.2639	1.52×10^{-4}	0.020
8.0	0.0170	0.2482	8.90×10^{-5}	0.002

Ac susceptibility measurements for Zn^{II}-doped samples: **3'$_{0.67}$**.

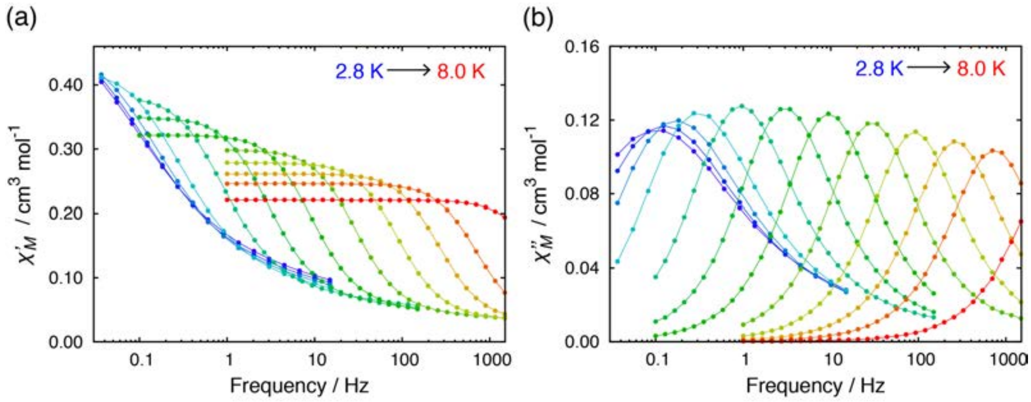

Fig. S28 Temperature dependence of (a) the in-phase χ'_M vs. frequency plots and (b) out-of-phase χ''_M vs. frequency plots for **3'$_{0.67}$** in 0 kOe dc field with ac frequency of 0.03–1488 Hz (2.8 K–8.0 K). The lines are a guide for the eye.

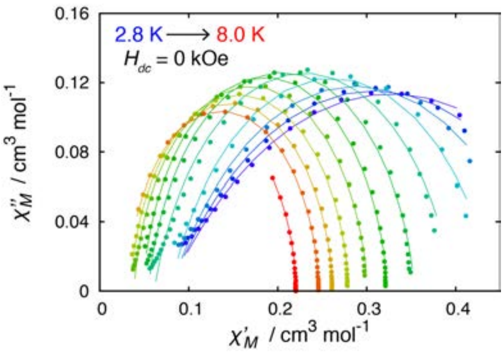

Fig. S29 Cole-Cole plot for **3'$_{0.67}$** in zero field from 2.8 to 8 K. The solid lines represent the fit to a generalized Debye model.

Table S19 Cole-Cole fit values for **3'$_{0.67}$** in zero dc field from 2.8 to 8.0 K.

T / K	χ_S / cm3 mol^{-1}	χ_T / cm3 mol^{-1}	τ / s	α
2.8	0.0769	0.5789	1.71×10^{0}	0.459
3.0	0.0782	0.5393	1.27×10^{0}	0.409
3.2	0.0796	0.4967	8.59×10^{-1}	0.344
3.5	0.0789	0.4444	4.58×10^{-1}	0.247
4.0	0.0612	0.3982	1.53×10^{-1}	0.185
4.5	0.0545	0.3543	4.87×10^{-2}	0.110
5.0	0.0484	0.3234	1.60×10^{-2}	0.070
5.5	0.0387	0.3012	5.12×10^{-3}	0.068
6.0	0.0344	0.2798	1.69×10^{-3}	0.052
6.5	0.0300	0.2618	5.79×10^{-4}	0.045
7.0	0.0272	0.2462	2.17×10^{-4}	0.035
8.0	0.0212	0.2202	4.03×10^{-5}	0.013

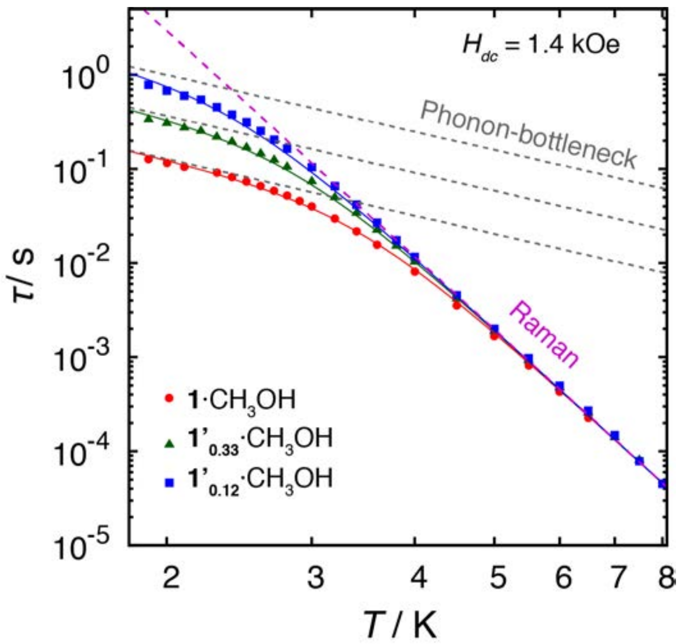

Fig. S30 Temperature dependence of the relaxation time τ for **1**·CH_3OH, **1'**$_{0.33}$·CH_3OH and **1'**$_{0.12}$·CH_3OH under 1.4 kOe dc field. The dashed lines indicate fitted lines for a single relaxation process of Raman $\tau^{-1} = CT^n$ and phonon-bottleneck limited direct process $\tau^{-1} = A_{pb}T^2$. The solid lines indicate the sum of the two relaxation processes.

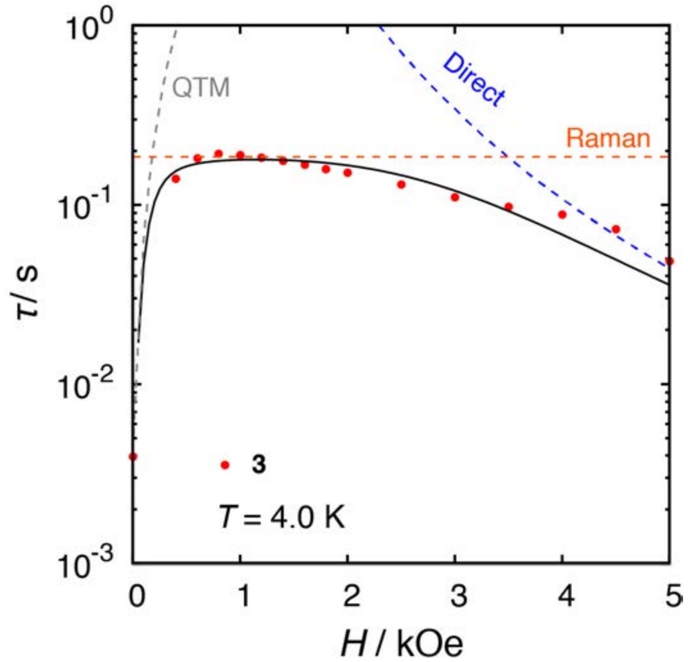

Fig. S31 Field dependence of the relaxation time τ for **3** at 4.0 K. The dashed lines indicate fitted lines for a single relaxation process of QTM $\tau^{-1} = B_1/(1+B_2H^2)$, Raman $\tau^{-1} = CT^n$ and direct process $\tau^{-1} = ATH^4$. The solid lines indicate the sum of the two relaxation processes.

Table S20 Fitting parameters for the relaxation dynamics in **1**·CH_3OH, **1’$_{0.33}$**·CH_3OH and **1’$_{0.12}$**·CH_3OH.

	H_{dc} / kOe	A_{pb} / $s^{-1}K^{-2}$	B_1 / s^{-1}	B_2 / kOe^{-2}	C / s^{-1} K^{-n}	n
1·CH_3OH	1.4	1.96			1.35×10^{-3}	8.0
1’$_{0.33}$·CH_3OH	1.4	6.84×10^{-1}			1.35×10^{-3}	8.0
1’$_{0.12}$·CH_3OH	1.4	2.51×10^{-1}	5006	46.3	1.35×10^{-3}	8.0

Table S21 Fitting parameters for the relaxation dynamics in **2** and **2’$_{0.52}$**.

	H_{dc} / kOe	C / s^{-1} K^{-}	n
2	0	1.18×10^{-2}	6.6
	0.4	1.18×10^{-2}	6.6
2’$_{0.52}$	0	1.18×10^{-2}	6.6

Table S22 Fitting parameters for the relaxation dynamics in **3** and **3’$_{0.67}$**.

	H_{dc} / kOe	A / kOe^{-4} s^{-1}	B_1 / s^{-1}	B_2 / kOe^{-2}	C / s^{-1} K^{-n}	n	τ_0 / s	Δ_{Orbach}/ cm^{-1}
3	0	9.05×10^{-3}	237.7	1361			2.40×10^{-10}	63.9
	0.8				4.69×10^{-4}	6.7	4.77×10^{-10}	63.9
3’$_{0.67}$	0				4.69×10^{-4}	6.7	4.77×10^{-10}	63.9

Table S23 Fitting parameters for the relaxation dynamics in **4**·CH_3OH.

	H_{dc} / kOe	τ_{QTM} / s	C / s^{-1} K^{-n}	n
4·CH_3OH	0	4.67×10^{-4}	4.68×10^{-2}	6.41
	0.4	1.43×10^{-3}	4.68×10^{-2}	6.41
	1.8	8.82×10^{-2}	4.68×10^{-2}	6.41

3. Powder X-ray diffraction measurement.

Powder XRD data was collected at room temperature on a Rigaku RINT 2100 powder diffractometer using Cu Kα radiation (λ = 1.5418 Å). The sample was ground in an agate mortar and placed on a silicon sample holder. The simulated powder pattern was calculated from the cif using the Mercury 3.8 software.

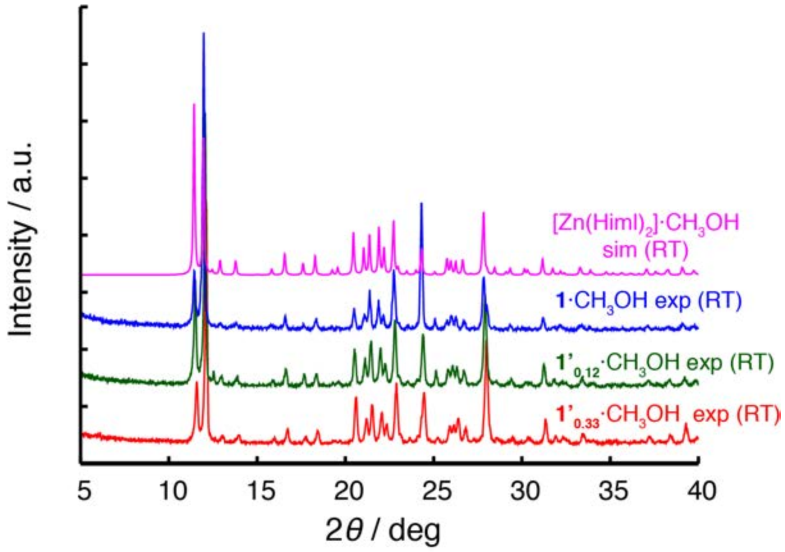

Fig. S32 Powder XRD patterns of **1**·CH_3OH, **1'$_{0.12}$**·CH_3OH, **1'$_{0.33}$**·CH_3OH and the simulated pattern of [Zn(Himl)$_2$]·CH_3OH at room temperature.**Error! Bookmark not defined.**

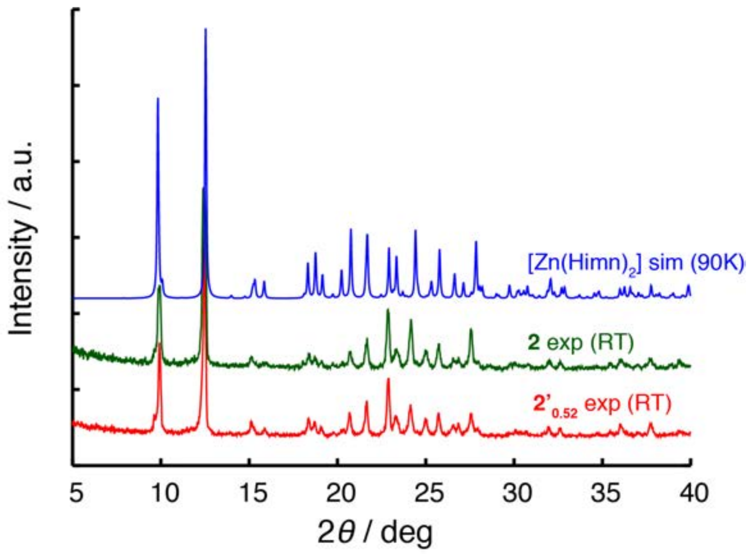

Fig. S33 Powder XRD patterns of **2** and **2'$_{0.52}$** at room temperature, and the simulated pattern of [Zn(Himn)$_2$] at 90 K.[2]

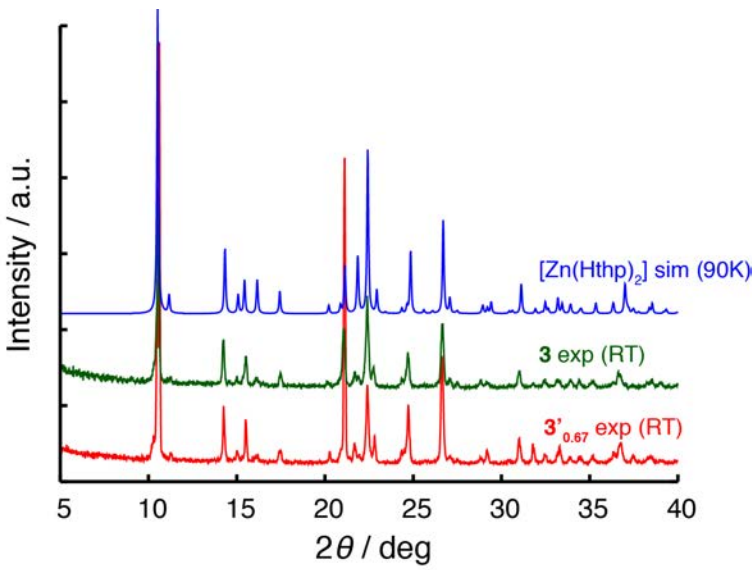

Fig. S34 Powder XRD patterns of **3** and **3'$_{0.67}$** at room temperature, and the simulated patterns of $[Zn(Hthp)_2]$ at 90 K.[3]